Journal of Petroleum Research and Studies

Open Access
Vol. 15, No. 2, June 2025, pp. 44-59

P- ISSN: 2220-5381
E- ISSN: 2710-1096

DOI: http://doi.org/10.52716/jprs.v15i2.1072

AI-Based Estimation of Poisson's Ratio for Carbonate Formations Using Drilling Parameters in a Southern Iraqi Oil Field

Doaa S. Mahdi[1], Emad A. Al-Khdheeawi[1], Yujie Yuan[2, 3]

[1]Oil and Gas Engineering Department, University of Technology, Baghdad, Iraq.
[2]School of Earth Sciences, Yunnan University, Kunming 650500, Yunnan, China.
[3]School of Engineering, Edith Cowan University, Joondalup, WA 6027, Australia.
*Corresponding Author E-mail: yujieyuan@ynu.edu.cn, 150070@uotechnology.edu.iq

Received 23/01/2025, Revised 23/02/2025, Accepted 24/02/2025, Published 22/06/2025

Abstract

Wellbore instability is a significant issue encountered during drilling operations. The mechanical properties of the formation are among the many factors that affect wellbore instability. Poisson's ratio is one of these mechanical properties and is a key factor in mechanical earth modeling (GEM). It is extremely important to minimize risks in drilling and production operations like sand output, collapse, tight holes, and pipe sticking. Poisson's ratio estimation contributes to optimizing hydro-carbon recovery and making important choices for a suitable field development plan. Poisson's ratio (υ) can be estimated both statically and dynamically. Static techniques measure the static properties in the lab, although static techniques are thought to be the most accurate way to determine the Poisson's ratio, they are costly, time-consuming, and unable to produce a continuous profile for Poisson's ratio. At the same time, dynamic methods compute the dynamic properties from well logging, such as density and the velocities of the compressional and shear waves, which are not always available. Thus, in this study, an artificial intelligence (AI) model is developed to estimate the Poisson's ratio for carbonate formation in the southern Iraqi oil field using available parameters during drilling. The dataset used in this study comprises over 451 data points, which range from depth of 2228 to 2453 m for the operations of training and testing. These data are including weight on bit (WOB), rotary speed (RPM), mud flow rate (FLW), Torque (T), standpipe pressure (SPP), and rate of penetration (ROP). The results indicate that new model can predict the Poisson's ratio with a high degree of accuracy (i.e., 93% correlation coefficients). Predicting rock Poisson's ratio from drilling data enables the early construction of a geomechanical model and saves cost and time compared to laboratory testing.

Keywords: Poisson's Ratio; Carbonate rock; Artificial Neural Network, Drilling data, Well logging.

Open Access
Vol. 15, No. 2, June 2025, pp. 44-59

P- ISSN: 2220-5381
E- ISSN: 2710-1096

التقديرالقائم على الذكاء الاصطناعي لنسبة بواسون لتكوينات الكربونات بأستخدام معاملات الحفر في حقل نفطي بجنوب العراق

الخلاصة:

عدم استقرار البئر هو مشكلة كبيرة تواجهها عمليات الحفر. وتعتبر الخصائص الميكانيكية للتكوين من بين العوامل العديدة التي تؤثر على عدم استقرار البئر. وتعتبر نسبة بواسون واحدة من هذه الخصائص الميكانيكية وهي عامل رئيسي في النمذجة الميكانيكية للأرض (GEM). وهي مهمة للغاية لتقليل المخاطر في عمليات الحفر والإنتاج مثل إنتاج الرمال والانهيار والثقوب الضيقة وتوقف الأنابيب. ويساهم تقدير نسبة بواسون في تحسين استرداد الهيدروكربون واتخاذ خيارات مهمة لخطة تطوير الحقل المناسبة. ويمكن تقدير نسبة بواسون (υ) بشكل ساكن وديناميكي. وتقيس التقنيات الساكنة الخصائص في المختبر، ورغم أن التقنيات الساكنة تعتبر الطريقة الأكثر دقة لتحديد نسبة بواسون، إلا أنها مكلفة وتستغرق وقتًا طويلاً وغير قادرة على إنتاج قياسات مستمرة لنسبة بواسون مع عمق البئر. وفي الوقت نفسه، تحسب الطرق الديناميكية الخصائص الديناميكية من مجسات البئر، مثل الكثافة وسرعات الموجات الانضغاطية والقصية، والتي لا تتوفر دائمًا. لذلك في هذه الدراسة تم تطويرموديل للذكاء الاصطناعي (AI) لتقدير نسبة بواسون لتكوين الكربونات في حقل النفط جنوب العراق باستخدام البيانات المتاحة أثناء الحفر. تتألف مجموعة البيانات المستخدمة في هذه الدراسة من أكثر من 451 نقطة، تتراوح من عمق 2228 إلى 2453 مترًا لعمليات التدريب والاختبار. تتضمن هذه البيانات الوزن على الدقاقة (WOB) ، وسرعة الدوران(RPM) ، ومعدل تدفق الطين(FLW) ، وعزم الدوران(T) ، وضغط الأنبوب (SPP)، ومعدل الاختراق (ROP). تشير النتائج إلى أن النموذج الجديد يمكنه التنبؤ بنسبة بواسون بدرجة عالية من الدقة (أي معاملات ارتباط 93%). يتيح التنبؤ بنسبة بواسون للصخور من بيانات الحفر البناء المبكر للموديل الجيوميكانيكي ويوفر التكلفة والوقت مقارنة بالقياسات المختبرية.

1. Introduction

Wellbore instability is one of the main issues engineers face when drilling and it can lead to various drilling issues such as tight boreholes, lost circulation, pipe sticking, and bit balling [1,2]. It is common to attribute the causes of wellbore instability to mechanical effects. Changes in the in situ stresses surrounding the wellbore or improper drilling techniques are the main causes of mechanical failure [3,4].

To provide practical solutions for mechanically induced wellbore stability issues, it is crucial to determine Poisson's ratio, which represents the elastic behavior of rock [5–8].

Poisson's ratio (υ) is defined by the International Society for Rock Mechanics and Rock Engineering (ISRM) as the ratio of longitudinal strain to lateral strain after a rock specimen is subjected to a deforming force below the proportionality limit [9]. Poisson's ratio varies with lithology and related rock characteristics like temperature, fluid saturation, bulk density, porosity, and rock consolidation [10].

Poisson's ratio can be measured using two primary methods: dynamic and static methods. Assessing the static Poisson's ratio (υ_{st}) requires performing destructive laboratory tests by applying relatively high static stresses to rock samples. This static loading test yields stress and

Open Access
Vol. 15, No. 2, June 2025, pp. 44-59

P- ISSN: 2220-5381
E- ISSN: 2710-1096

stain data that are used to determine important mechanical parameters, such as compressive strength, Young's modulus, and Poisson's ratio. For a test, the Poisson's ratio equation is as follows [11,12]:

$$\boldsymbol{v_{st}} = -\frac{\boldsymbol{lateral\ Strain}}{\boldsymbol{Axial\ Strain}} \qquad (1)$$

The value provided by Equation (1) varies with the amount of stress, and the slope of stress-strain curves generally changes as stress increases.

However, the dynamic Poisson's ratio is obtained by utilizing well log data for the entire well, such as sonic log, as follows [13]:

$$\boldsymbol{v_{dyn}} = \left(\frac{v_p{}^2 - 2v_s{}^2}{2(v_p{}^2 - v_s{}^2)}\right) \qquad (2)$$

Where: V_S is the shear wave speed, V_P is the compressional wave speed, and ν_{dyn} is the dynamic Poisson's ratio.

The response of rocks' static Poisson's ratio to stresses can differ significantly from that inferred from dynamic wave measurements [14]. Therefore, it is important to note that the values of the dynamic and static elastic parameters typically vary. One of the main causes of this discrepancy is the existence of microcracks in the rock. The dynamic and static Poisson's ratios for metallic samples without cracks are nearly equal [15]. Moreover, dynamic loading induces elastic strains, whereas static tests result in a portion of strains that are irrecoverable. These additional factors contribute to the disparity between dynamic and static Poisson's ratio. Poisson's ratio is employed in petroleum engineering in various applications. Rock core samples must be taken from the formation for this purpose, which makes them very costly. On the other hand, any engineering operation requires a continuous profile of Poisson's ratio. Table (1) presents AI models that were used to construct the correlations.

Table (1): Previous AI-developed models for the Poisson's ratio

Input parameters	Data points	Reference
V_S, V_P, density	77	[16]
V_S,V_P, density.pore pressure	602	[17]
V_S, V_P, density	610	[18]
V_S, V_P, density, gammaray, porosity	580	[19]

Open Access
Vol. 15, No. 2, June 2025, pp. 44-59

P- ISSN: 2220-5381
E- ISSN: 2710-1096

The majority of these models used formation porosity (Ø) and sonic transit time (Dt) to determine the Poisson's ratio. However, when drilling the wellbore, such well-log data are not always accessible because they are frequently acquired by a wireline logging technique, which is typically carried out following wellbore drilling in order to prevent the harsh drilling environment [20]. Importantly, drilling parameters have advantages over well logging data including its availability and cost effective [21]. Thus, this study proposes to replace well logs with drilling data to estimate Poisson's ratio.

Therefore, the primary goal of this study is to present a new ANN model for forecasting the Poisson's ratio as function of drilling parameters.

1.1. Area of Study Geological Description

Regarding petroleum reserves, the Mesopotamian Basin is among the most abundant basins in the world Figure (1) [22]. The Cretaceous carbonate layers contain a significant amount of oil imprisoned within the basin Figure (2) [23]. The Mesopotamian Basin's carbonate sequence can be classified into packages based on the highest flooding surfaces and regional-scale discrepancies. Using these surfaces, the Mesopotamian Basin's early Turonian and late Albian rocks were grouped into one megasequence [24]. At the top of this mega-sequence is the Mishrif Formation, which is covered by the Khasib Member with an intense interaction that indicates an early-middle Turonian discrepancy [25]. At its lowest point limit, however, the Mishrif Formation gradually transitions into the Rumaila Formation underneath it, and in several wells, it is difficult to distinguish between the two formations [24]. The Mishrif Formation consists of detrital and bioclastic lime-stones and has reservoir porosity greater than 0.2 and permeability range of 0.1 to 1 Darcy and it is considered as the greatest significant oil reserve in the Mesopotamian Basin[26]. The Mishrif Formation extends across the Mesopotamian Basin, reaching depths of approximately 2100–2400 meters in the Basrah District and thicknesses of 100–200 meters. However, Marly and Chalky limestones make up the majority of the Rumaila Formation underneath Mishrif. Rumaila Formation is a Cenomanian-aged member of the Waisa Group and serves as a significant reservoir in the northern, central, and southern Mesopotamian Basins.

Journal of Petroleum Research and Studies

Open Access
Vol. 15, No. 2, June 2025, pp. 44-59

P- ISSN: 2220-5381
E- ISSN: 2710-1096

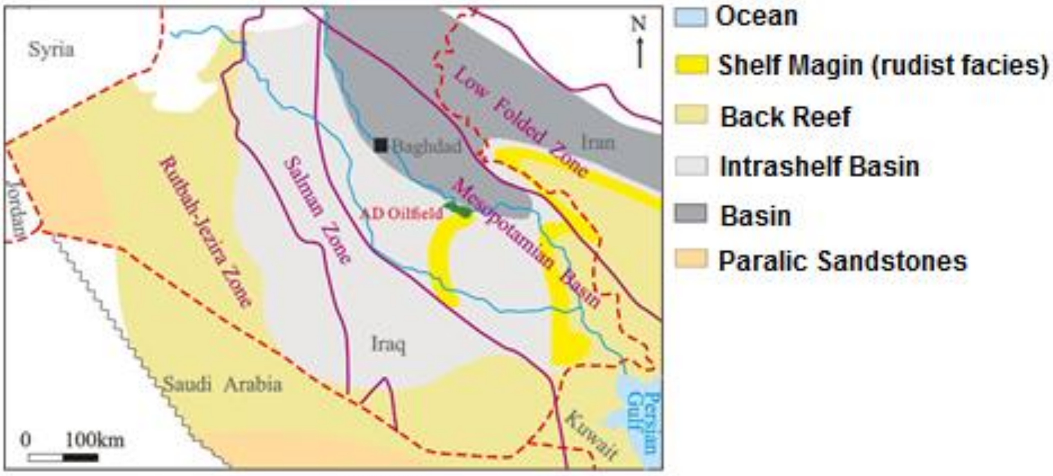

Fig. (1): Tectonic zoning, the Late Cenomanian paleogeographic information, along with the study area's location

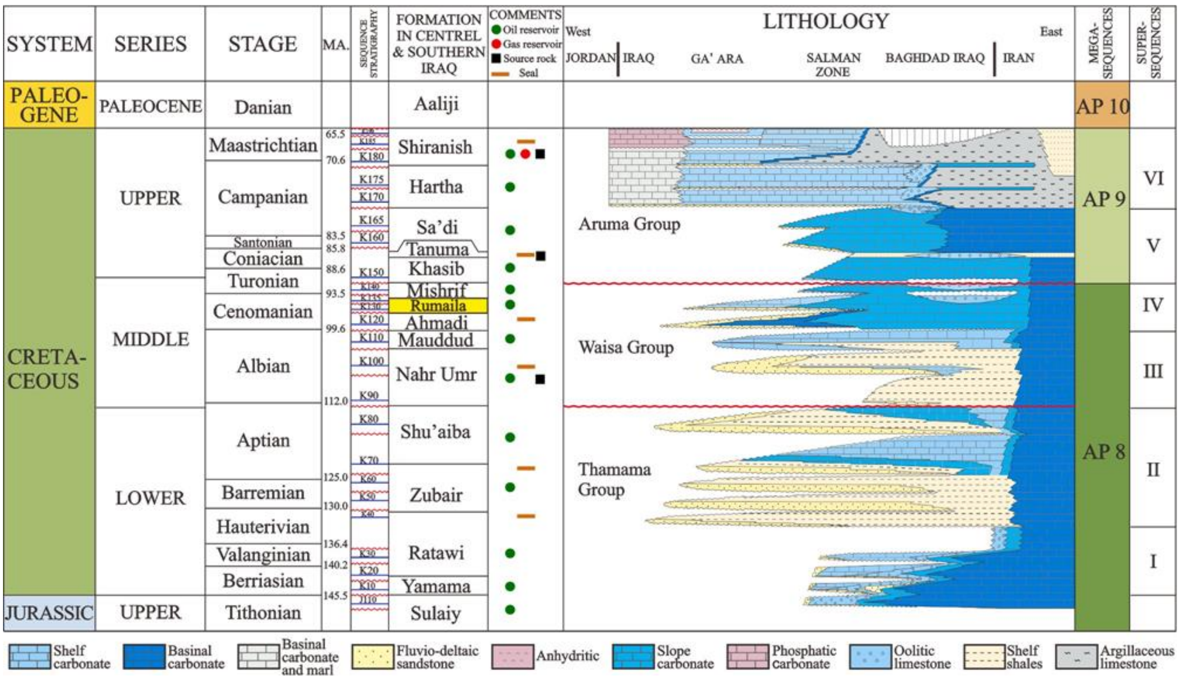

Fig. (2): Petroleum system components, sequence stratigraphic structure, lithostratigraphy, and chronostratigraphy of Mesopotamian Basin

2. Methodology

2.1. Artificial Neural Network

Artificial neural network (ANN) aids in the identification and classification of intricate systems that are too difficult for the human brain to understand [27–30]. We chose the ANN model for this study because it can autonomously organize algorithms, leading to accurate

Open Access
Vol. 15, No. 2, June 2025, pp. 44-59

P- ISSN: 2220-5381
E- ISSN: 2710-1096

results, in contrast to other machine learning techniques that depend on learned data for decision-making [31]. Neural networks typically contain three distinct layer types: input, hidden, and out-put layers. A set of weights and biases connects these layers, which are modified as the network is optimized to control the network's prediction efficiency [32]. Only transmitting the input data to the hidden layer is the input layer's job. Without performing any calculations. The weighted sum of a neuron's input is subjected to a transfer function to ascertain the neuron's output [33]. Figure (3) shows the methodology used in this study to correlate drilling parameters with Poisson's ratio.

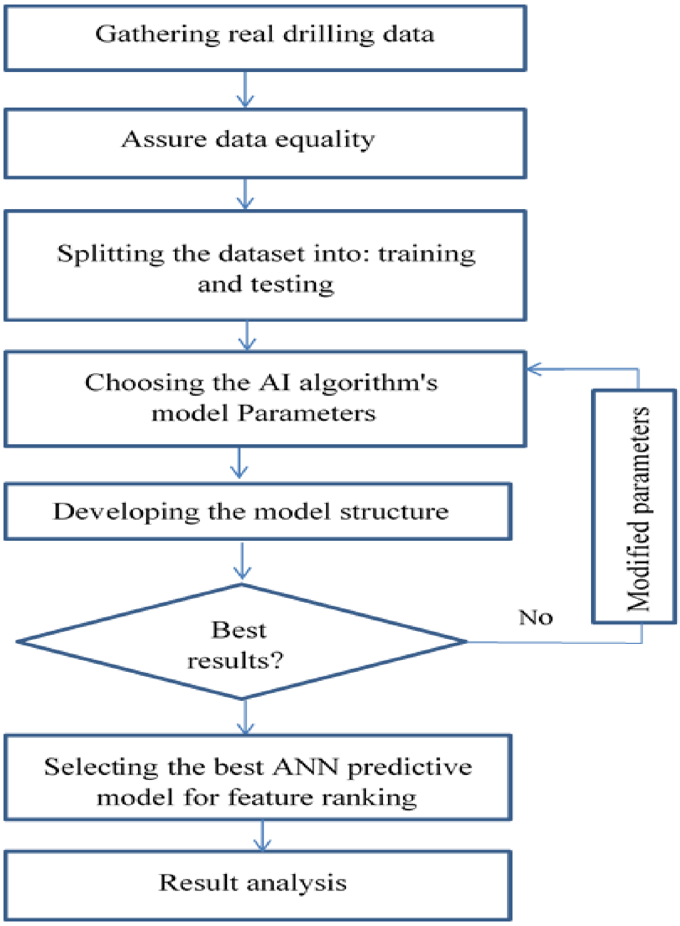

Fig. (3): Flow chart for ANN model prediction Poisson's ratio

2.2. Data Description

An 8.5-inch section of an oil well located in the Mesopotamian Basin will be the area of this paper's investigation. The Mishrif and Rumaila carbonate formations provided the study's data that ranged in depth from 2228 to 2453 meters with a set of 451 data points. Drilling variables

Open Access
Vol. 15, No. 2, June 2025, pp. 44-59

P- ISSN: 2220-5381
E- ISSN: 2710-1096

are regularly recorded at the surface using precise real-time sensors to monitor drilling performance during operations used in this study weight on bit (WOB), flow rate (FLW), speed of penetration (ROP), Torque (T), revolutions per minute (RPM), and standpipe pressure (SPP). Poisson's ratio is obtained from well log data for the same depths of the drilling variables measurements using Equation (2). The data was preprocessed to remove outliers before machine learning model was created. To start, the drilling data were filtered to eliminate clear outliers and situations in which drilling was stopped.

The degree to which the two factors are linearly related was determined using the correlation coefficient (CC) to assess how strongly Poisson's ratio and the drilling data are related. The range of its value is -1 to 1. When the CC-value is 1, it indicates that the relationships are strong. However, reverse linear correlation is indicated by a CC-value of -1. On the other hand, the CC-value of zero, on the other hand, indicates that the two study parameters are unrelated. Figure (5) shows the relative importance of the output parameter (Poisson's ratio) and the input parameters individually in terms of CC-value. The correlation coefficient's main drawback is the presumption of a relationship that is linear. Additionally, if the dependent or independent variables are scaled or modified linearly, the correlation coefficient will stay unchanged. However, a low correlation coefficient may result from a non-linear connection between dependent or independent variables, even though they clearly demonstrate a relationship. Because of non-linear relation-ships, the correlation coefficient might not always equal zero. A correlation coefficient evaluates how closely observations match a single straight line rather than concentrating on the best-fit line. Figure (4) presents the correlation coefficient for each drilling variable with Poisson's ratio. Figure (5) illustrates how Poisson's ratio varies with the studied drilling variables (i.e. WOB, ROP, FLW, Torque, RPM, and SPP). It revealed that the dataset showed good representation and data spread across a wider range of drilling parameters.

Open Access
Vol. 15, No. 2, June 2025, pp. 44-59

P- ISSN: 2220-5381
E- ISSN: 2710-1096

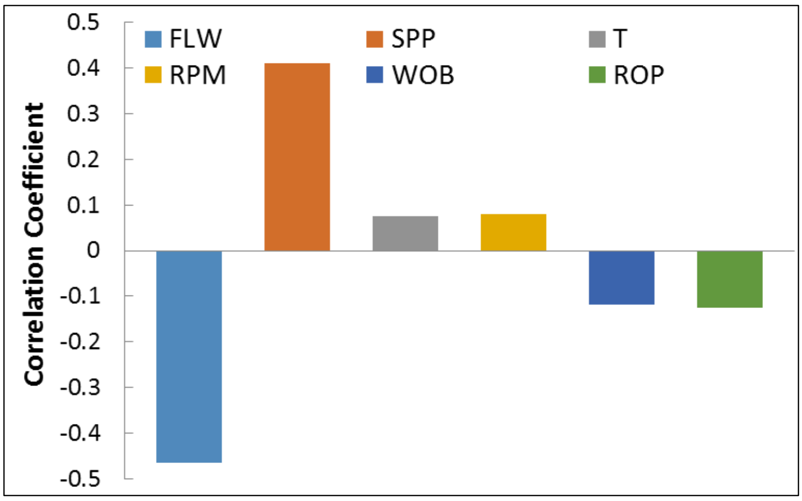

Fig. (4): Correlation coefficient between the Poisson's ratio the drilling variables

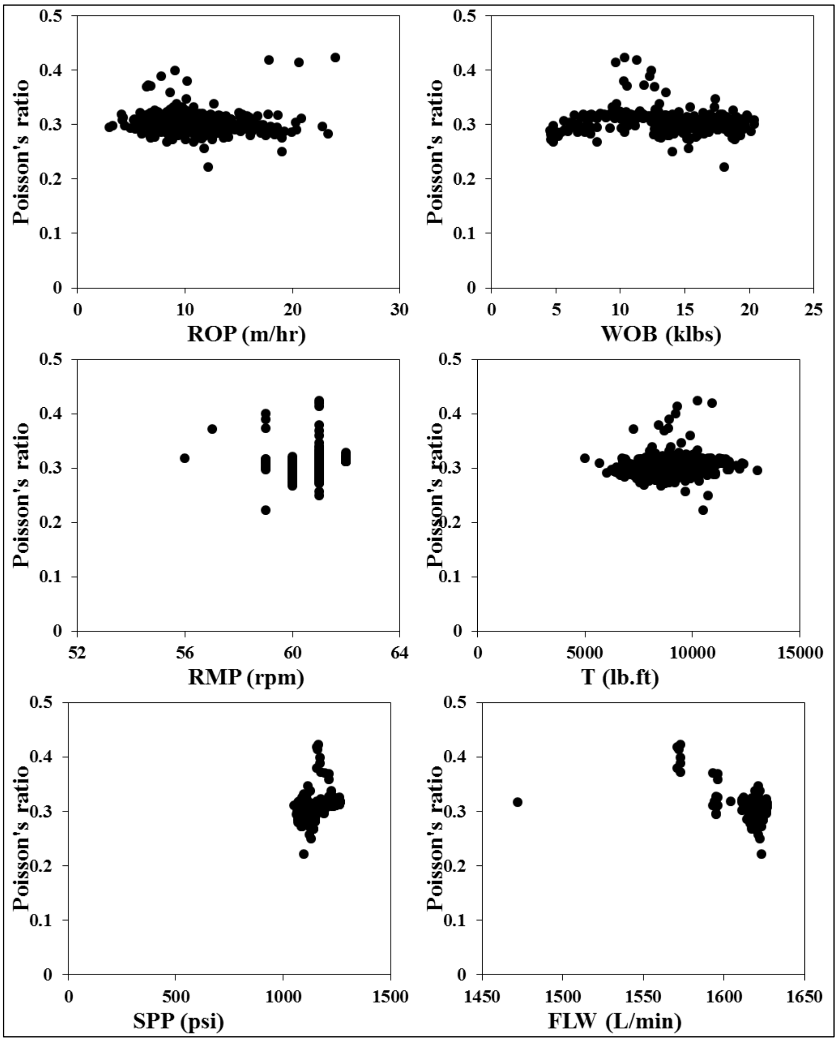

Fig. (5): Variation Poisson's ratio as a function of the different investigated drilling variables

Open Access
Vol. 15, No. 2, June 2025, pp. 44-59

P- ISSN: 2220-5381
E- ISSN: 2710-1096

3. Results and Discussion

In order to develop the new model for predicting Poisson's ratio and because the input (drilling data) and output data (Poisson's ratio) have different ranges, a normalization process has been applied to them before the new ANN model's training and testing process begins. The data is normalized to a predefined range from its domain using the Min-Max normalization technique [34]. This technique entails rescaling the attribute from its initial range to a new range, such as 0 to 1. The formulation of this method is as follows:

$$\mathbf{XI} = \frac{(\boldsymbol{X - Xmin})}{(\mathbf{Xmax - Xmin})} \tag{3}$$

Where: Xmin is the lowest value of each parameter, Xmax is the maximum value of each parameter, XI is the value following normalization, and X is the original value for each data point. The Poisson's ratio ANN model employed six input variables, including torque (T), mud flow rate (FLW), standpipe pressure (SPP), rotary speed (RPM), weight on bit (WOB), and rate of penetration (ROP). Following that, the dataset is split into 70% (318 data points) and 30% (133 data points) at random for training and testing the model, respectively. A back-propagation algorithm was employed to model the Poisson's ratio. The results indicate that the best number of neurons for the hidden layer of the developed model is nine. The other characteristics of the developed model are shown in Table (2).

Table (2): Poisson's ratio ANN model features

Property	Poisson's ratio Model
Input	6(T,FLW,SPP,RPM,WOB,and ROP)
Output	1 (Poisson's ratio)
Hidden layer	1
Hidden layer's Neuron	9
Goal	1.0000e-07
Transfer function	tansig
Train function	Trainlm
Training data points	318
Testing data points	133

The results of the training process (318 data points) for the new model for Poisson's ratio prediction are shown in Figure (6), which compares the predicted and measured Poisson's ratio. With a correlation coefficient (R) of 0.93, the new ANN model's ability to predict the Poisson's ratio is evident.

Open Access
Vol. 15, No. 2, June 2025, pp. 44-59

P- ISSN: 2220-5381
E- ISSN: 2710-1096

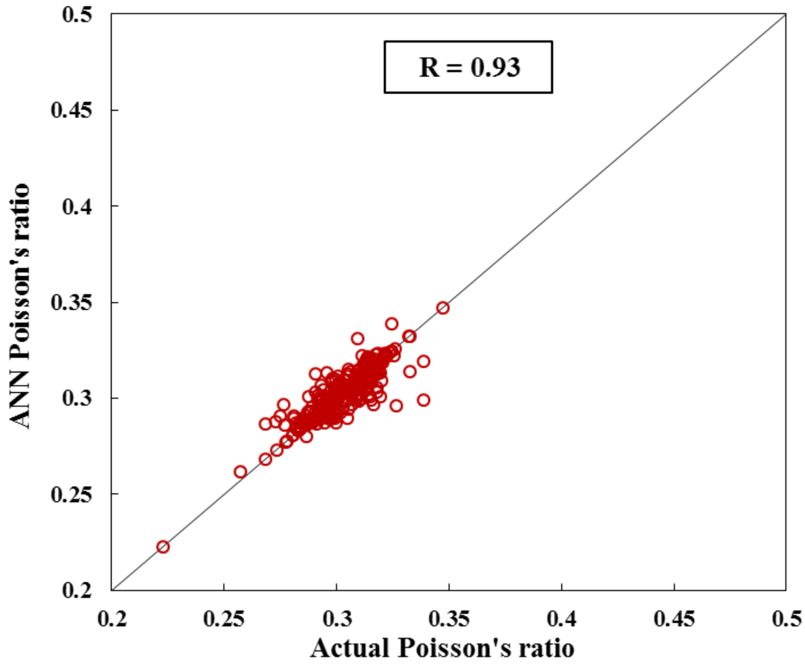

Fig. (6): Poisson's ratio prediction results for the training data (318 samples)

Additionally, after training, the model is tested using 133 data points that were absent during training. Figure (7) displays the result of the testing process. As can be seen from the correlation coefficient value (R = 0.88), the new ANN model estimates Poisson's ratio with a high degree of accuracy.

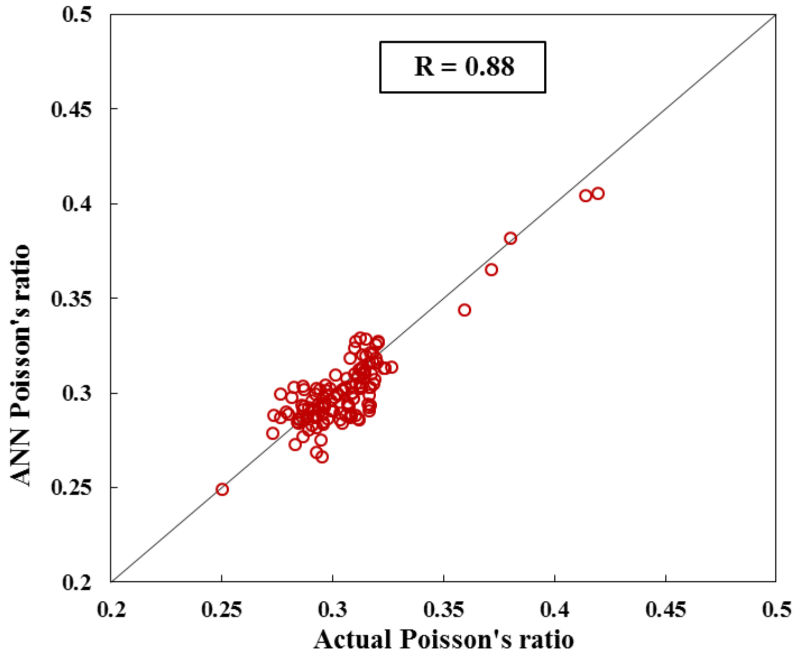

Fig. (7): Poisson's ratio prediction results for the testing data (133 samples)

Open Access
Vol. 15, No. 2, June 2025, pp. 44-59

P- ISSN: 2220-5381
E- ISSN: 2710-1096

The following empirical relationship for Poisson's ratio prediction is found after the final ANN model is created, and it may be applied to any future tasks that employ identical data extend as the present research without requiring the use of complicated ANN techniques:

$$\boldsymbol{PR_N} = \sum_{i=1}^{9} \boldsymbol{wk_j}\left(\frac{\mathbf{2}}{\mathbf{1}+e^{-2\left(w_{1i}\,ROP_N + w_{2i}\,WOB_N + w_{3i}\,RPM_N + w_{4i}\,T_N + w_{5i}\,SPP_N + w_{6i}\,FLW_N + b_i\right)}} - \mathbf{1}\right) + \boldsymbol{b_k} \qquad (3)$$

PR_N: normalized Poisson's ratio, i: hidden layer neurons, w1i, w2i, w3i, w4i, w5i, and w6i: weights between input and hidden layers for ROP, WOB, RPM, T, SPP, and FLW, respectively, subscript, wkj: weights between hidden and output layers, bi: bias of hidden layer, and bk: bias of output layer. Table (3) presents the weights and bias results of for the new model of Poisson's ratio. Denormalization is applied to the output parameter in order to precisely predict Poisson's ratio using the proposed correlation, and the resulting equation for Poisson's ratio is as follows:

$$\boldsymbol{Poisson's\ Ratio} = \mathbf{0.2015076}\,\boldsymbol{PR_N} + \mathbf{0.2226783} \qquad (4)$$

Table (3) Bias and weights for the created Poisson's ratio model

Neurons of Hidden Layer (j)	Input to Hidden Layers weights (w_{ij}); i = 1 to 6 for ROP, WOB, RPM, T, SPP, and FLW, respectively						Hidden Layer Bias (b_j)	Hidden to output Layers weights (wk_j)	Output Layer Bias (b_k)
	ROP	WOB	RPM	T	SPP	FLW			
1	-3.1831	-3.6714	-14.4775	0.71262	18.4092	0.078716	-6.6335	-0.0552	
2	0.7156	-7.6906	-1.192	3.0659	-4.4118	-1.1162	4.363	5.8696	
3	-8.3893	-20.8366	-3.9527	5.8835	16.9391	15.695	3.6619	-0.1654	
4	1.0295	7.2633	2.4736	-11.527	9.1014	6.2216	6.143	-0.6764	
5	-0.09732	0.038609	-0.03534	-0.0293	0.2122	0.08002	-0.69684	2.2002	1.613
6	39.9475	10.7839	7.0625	14.3015	-9.6226	-11.2761	4.5314	5.8752	
7	-36.7366	-9.6556	-4.6391	-13.5165	9.1524	10.1623	-4.6734	5.9101	
8	-24.5742	-4.4131	-7.3674	7.3538	-6.8711	-2.7684	-5.1736	-0.0779	
9	0.79725	-7.9648	-1.115	3.1546	-4.5924	-1.0321	4.3883	-5.7327	

Figure (8) compares the measured and predicted Poisson's ratio profiles. It is clear that the well log-based Poisson's ratio profile of the examined oil well section closely matches the expected Poisson's ratio profile for both training and testing processes. Taking everything into account, we determine that the newly created model accurately predicts the PR from drilling data for the formation under study.

Open Access
Vol. 15, No. 2, June 2025, pp. 44-59

P- ISSN: 2220-5381
E- ISSN: 2710-1096

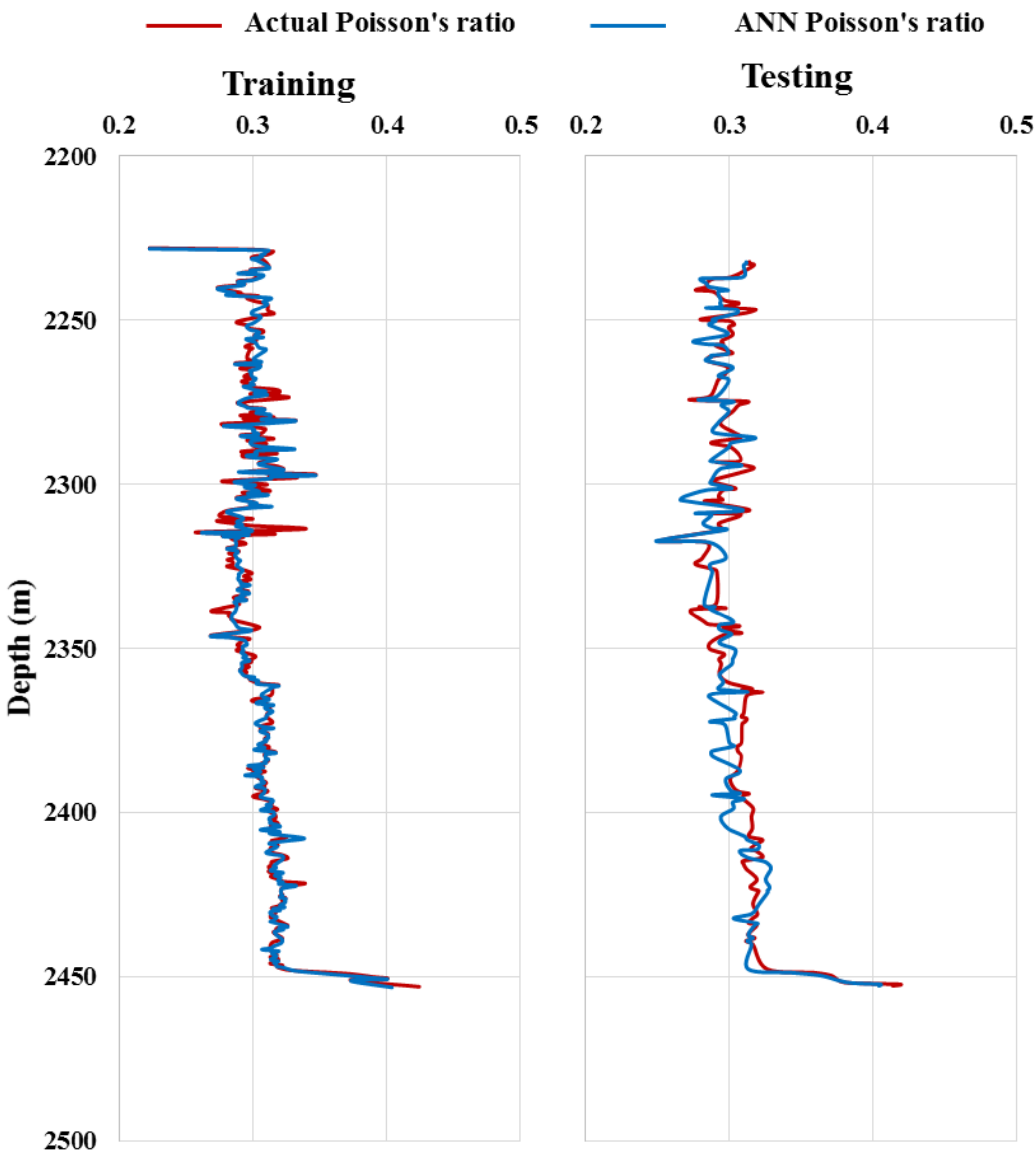

Fig. (8): Comparison of the measured and predicted Poisson's ratio profiles training and testing processes

4. Conclusions

It is essential to comprehend the geomechanical properties to mitigate well-bore stability issues and geomechanical modeling. One such geomechanical parameter is Poisson's ratio. This study suggests a new method for accurately and economically estimating the passion ratio values of downhole formations during drilling. Poisson's ratio prediction from drilling data is a helpful technique for engineers because drilling parameters are readily available and are an early type of information. This can help in enhancing the drilling efficiency, and decreasing the risk during drilling new formations.

Open Access
Vol. 15, No. 2, June 2025, pp. 44-59

P- ISSN: 2220-5381
E- ISSN: 2710-1096

The range of Poisson's ratio and drilling data used in this study are (0.22 to 0.42) for Poisson's ratio, (5000 to 13025 lb.ft) for torque, (4.56 to 20.4 klbs) for weight on bit, (1472 to 1627 L/mn) for flow rate, (56 to 62 rpm) for rotary speed, (1050 to 1264 psi) for standpipe pressure, and (2.99 to 23.98 m/h) for rate of penetration.

The final models were created using a dataset of 451 points, which was collected from 8.5 in an oil well section with depths from 2228 to 2453m for training and testing purposes. The new Poisson's ratio model has a 93% correlation coefficient, which indi-cates that it can predict the Poisson's ratio with reasonable accuracy. Thus, we conclude that when applied to a dataset that is within the same range as the data used to train the new model, the performance of the developed models to predict Poisson's ratio is assured.

Open Access
Vol. 15, No. 2, June 2025, pp. 44-59

P- ISSN: 2220-5381
E- ISSN: 2710-1096

References

[1] M. Mohiuddin, K. Khan, A. Abdulraheem, and A. Al-Majed, “Analysis of wellbore instability in vertical, directional, and horizontal wells using field data”, *J. Pet. Sci. Eng.*, vol. 55, no. 1-2, pp. 83–92, 2007. https://doi.org/10.1016/j.petrol.2006.04.021.

[2] T. M. Al-Bazali, J. Zhang, C. Wolfe, M. E. Chenevert, and M. M. Sharma, “Wellbore instability of directional wells in laminated and naturally fractured shales”, *J. Porous Media*, vol. 12, no. 2, pp. 119-130, 2009. https://doi.org/10.1615/JPorMedia.v12.i2.20.

[3] N. W. Tschoegl, W. G. Knauss, and I. Emri, “Poisson’s ratio in linear viscoelasticity – A critical review”, *Mechanics of Time-Dependent Materials*, vol. 6, pp. 3–51, 2002. https://doi.org/10.1023/A:1014411503170.

[4] M. E. Zeynali, “Mechanical and physico-chemical aspects of wellbore stability during drilling operations”, *Journal of Petroleum Science and Engineering*, vol. 82-83, pp. 120–124, 2012. https://doi.org/10.1016/j.petrol.2012.01.006

[5] M. Aslannezhad, A. Keshavarz, and A. Kalantariasl, “Evaluation of mechanical, chemical, and thermal effects on wellbore stability using different rock failure criteria”, *Journal of Natural Gas Science and Engineering*, vol. 78, p. 103276, 2020. https://doi.org/10.1016/j.jngse.2020.103276.

[6] V. Maury, “Rock failure mechanisms identification: A key for wellbore stability and reservoir behaviour problem”, presented at the *SPE/ISRM Rock Mechanics in Petroleum Engineering*, p. SPE-28049-MS, 1994. https://doi.org/10.2118/28049-MS.

[7] C. J. Nmegbu and L. V. Ohazuruike, “Wellbore instability in oil well drilling: A review”, *International Journal of Engineering Research and Development*, vol. 10, no. 5, pp. 11–20, 2014.

[8] S. V. Dmitriev, T. Shigenari, and K. Abe, “Poisson ratio beyond the limits of the elasticity theory,” *Journal of the Physical Society of Japan*, vol. 70, no. 5, pp. 1431–1432, 2001. https://doi.org/10.1143/jpsj.70.1431.

[9] L. E. Malvern, “Introduction to the Mechanics of a Continuous Medium”, Paper No. Monograph, 1969.

[10] K. K. Phani, “Correlation between ultrasonic shear wave velocity and Poisson’s ratio for isotropic porous materials”, *Journal of materials science*, vol. 43, pp. 316–323, 2008. https://doi.org/10.1007/s10853-007-2055-2

[11] J. Kumar, “The effect of Poisson's ratio on rock properties”, presented at the *SPE Annual Fall Technical Conference and Exhibition*, p. SPE-6094-MS, 1976. https://doi.org/10.2118/6094-MS.

[12] G. N. Greaves, A. L. Greer, R. S. Lakes, and T. Rouxel, “Poisson’s ratio and modern materials,” *Nature Materials*, vol. 10, pp. 823–837, 2011. https://doi.org/10.1038/nmat3134.

[13] R. D. Barree, J. V. Gilbert, and M. Conway, “Stress and rock property profiling for unconventional reservoir stimulation”, presented at the *SPE Hydraul. Fract. Tech. Conf.*, 2009. SPE-118703-MS. https://doi.org/10.2118/118703-MS.

Open Access
Vol. 15, No. 2, June 2025, pp. 44-59

P- ISSN: 2220-5381
E- ISSN: 2710-1096

[14] M. Ciccotti and F. Mulargia, “Differences between static and dynamic elastic moduli of a typical seismogenic rock”, *Geophysical Journal International*, vol. 157, no. 1, pp. 474–477, 2004. https://doi.org/10.1111/j.1365-246X.2004.02213.x.

[15] Z. Wang and A. Nur, “Dynamic versus static elastic properties of reservoir rocks”, *Seismic and acoustic velocities in reservoir rocks*, vol. 3, pp. 531–539, 2000.

[16] A. Abdulraheem, “Prediction of Poisson’s ratio for carbonate rocks using ANN and fuzzy logic type-2 approaches,” presented at the *international petroleum technology conference*, p. IPTC-19365-MS, 2019. https://doi.org/10.2523/IPTC-19365-MS.

[17] B. D. Al-Anazi, M. T. Al-Garni, T. Muffareh, and I. Al-Mushigeh, “Prediction of Poisson’s ratio and Young’s modulus for hydrocarbon reservoirs using alternating conditional expectation algorithm”, presented at the *SPE Middle East Oil and Gas Show and Conf.*, Manama, Bahrain, p. SPE-138841-MS, 2011. https://doi.org/10.2118/138841-MS.

[18] S. M. Elkatatny, Z. Tariq, M. A. Mahmoud, Z. A. Abdulraheem Abdelwahab, M. Woldeamanuel, and I. M. Mohamed, “An artificial intelligent approach to predict static Poisson’s ratio”, presented at the *ARMA US Rock Mechanics/Geomechanics Symposium*, Paper Number: ARMA-2017-0771, USA, June 2017.

[19] Z. Tariq, A. Abdulraheem, M. Mahmoud, and A. Ahmed, “A rigorous data-driven approach to predict Poisson’s ratio of carbonate rocks using a functional network”, *Petrophysics*, vol. 59, no. 6, pp. 761–777, 2018. https://doi.org/10.30632/PJV59N6-2018a2.

[20] C. Chang, M. D. Zoback, and A. Khaksar, “Empirical relations between rock strength and physical properties in sedimentary rocks”, *Journal of Petroleum Science and Engineering*, vol. 51, no. 3-4, pp. 223–237, 2006. https://doi.org/10.1016/j.petrol.2006.01.003.

[21] O. Siddig, A. F. Ibrahim, and S. Elkatatny, “Estimation of rocks’ failure parameters from drilling data by using artificial neural network”, *Scientific Reports*, vol. 13, p. 3146, 2023. https://doi.org/10.1038/s41598-023-30092-2.

[22] D. L. Cantrell, R. A. Shah, J. Ou, C. Xu, C. Phillips, X. L. Li, and T. M. Hu, “Depositional and diagenetic controls on reservoir quality: Example from the Upper Cretaceous Mishrif Formation of Iraq”, *Marine and Petroleum Geology*, vol. 118, p. 104415, 2020. https://doi.org/10.1016/j.marpetgeo.2020.104415.

[23] E. W. Adams, C. Grélaud, M. Pal, A. É. Csoma, O. S. Al Ja'aidi, and R. A. Hinai, “Improving reservoir models of Cretaceous carbonates with digital outcrop modelling (Jabal Madmar, Oman): Static modelling and simulating clinoforms”, *Petroleum Geoscience*, vol. 17, no. 3, 2011. https://doi.org/10.1144/1354-079310-031.

[24] S. Iraji et al., “Laboratory and numerical examination of oil recovery in Brazilian pre-salt analogues based on CT images,” presented at the *3rd EAGE Conference on Pre Salt Reservoirs*, 2022.

[25] H. Al-Khersan, “Depositional environments and geological history of the Mishrif Formation in Southern Iraq”, *Proceeding at 4th Arab Petroleum Congress*, Dubai, 1975.

Open Access
Vol. 15, No. 2, June 2025, pp. 44-59

P- ISSN: 2220-5381
E- ISSN: 2710-1096

[26] A. Aqrawi, G. Thehni, G. Sherwani, and B. Kareem, “Mid-Cretaceous rudist-bearing carbonates of the Mishrif Formation: An important reservoir sequence in the Mesopotamian Basin, Iraq”, *Journal of petroleum Geology*, vol. 21, no. 1, pp. 57–82, 1998. https://doi.org/10.1111/j.1747-5457.1998.tb00646.x.

[27] Z. Huang, J. Shimeld, M. Williamson, and J. Katsube, “Permeability prediction with artificial neural network modeling in the Venture Gas Field, Offshore Eastern Canada”, *Geophysics*, vol. 61, no. 2, pp. 422–436, 1996. https://doi.org/10.1190/1.1443970.

[28] A. A. Del Castillo, E. Santoyo, and O. García-Valladares, “A new void fraction correlation inferred from artificial neural networks for modeling two-phase flows in geothermal wells”, *Computers & Geosciences*, vol. 41, pp. 25–39, 2012. https://doi.org/10.1016/j.cageo.2011.08.001.

[29] E. A. Al-Khdheeawi and D. S. Mahdi, “Apparent viscosity prediction of water-based muds using empirical correlation and an artificial neural network”, *Energies*, vol. 12, no. 16, p. 3067, 2019. https://doi.org/10.3390/en12163067.

[30] A. Abdulraheem, M. Ahmed, A. Vantala, and T. Parvez, “Prediction of rock mechanical parameters for hydrocarbon reservoirs using different artificial intelligence techniques”, presented at the *SPE Kingdom of Saudi Arabia Annual Technical Symposium and Exhibition*, p. SPE-126055-MS, 2009. https://doi.org/10.2118/126094-MS.

[31] D. S. Mahdi and E. A. Al-Khdheeawi, “A new model for optimizing drilling variables and penetration rate”, *AIP Conference Proceedings*, vol. 2443, no. 1, AIP Publishing, 2022. https://doi.org/10.1063/5.0091936.

[32] P. Panja, J. Goral, M. Deo, and J. McLennan, “Prediction of geomechanical properties from elemental analysis using machine learning algorithm”, presented at the *54th U.S. Rock Mechanics/ Geomechanics Symposium*, 2020.

[33] D. S. Mahdi, “Predicting drilling rate of penetration using artificial neural networks”, *IOP conference series: Materials science and engineering*, vol. 1067, p. 012150, 2021. https://doi.org/10.1088/1757-899X/1067/1/012150.

[34] A. S. Eesa and W. K. Arabo, “A normalization methods for backpropagation: A comparative study”, *Science Journal of University of Zakho*, vol. 5, no. 4, pp. 319–323, 2017. https://doi.org/10.25271/2017.5.4.381.